

Topological methods for searching barriers and reaction paths

Sorin Tănase-Nicola and Jorge Kurchan

*P.M.M.H. Ecole Supérieure de Physique et Chimie Industrielles,
10, rue Vauquelin, 75231 Paris CEDEX 05, France*

(Dated: November 1, 2018)

We present a family of algorithms for the fast determination of reaction paths and barriers in phase space and the computation of the corresponding rates. The method requires the reaction times be large compared to the microscopic time, irrespective of the origin — energetic, entropic, cooperative — of the timescale separation. It lends itself to temperature cycling as in simulated annealing and to activation-relaxation routines. The dynamics is ultimately based on supersymmetry methods used years ago to derive Morse theory. Thus, the formalism automatically incorporates all relevant topological information.

A situation often met in chemical reactions, protein folding and nucleation transitions is that the evolution breaks into fast local relaxations and rare *activation* processes. This timescale separation can be a consequence of low temperature (intra-valley equilibration occurs in $\tau_{fast} = O(1)$, passage times are exponential $\tau_{activ} \sim \exp(\Delta E/T)$), or of cooperative dynamics: e.g. in a ferromagnet of size L the relaxation time within a state $\tau_{fast} < L^2$ (the time for the largest domain to collapse), and between phases $\tau_{activ} \sim \exp(cL^{d-1})$. It can also be the result of *entropic barriers*, flat but narrow energy canyons that the system is unlikely to transit.

In all these cases, a knowledge of the actual connectivity of paths and saddles gives a global picture of a system's behavior [1]. Direct information on the barriers can also be used to model the activated processes, without the need to wait for them to occur spontaneously, thus allowing to simulate a reaction even faster than nature. Furthermore, *activation/relaxation* procedures [2], alternating ordinary relaxation with forced activation, offer an efficient way to sample phase-space. For these investigations, several algorithms [1, 2] have been implemented to locate saddle points in energy. In cases when the nature of barriers is qualitatively affected by entropy, one needs to study directly the transition probability — thus taking into account the multiplicity of paths through the (“free energy”) barrier. A well known method to do this is a MonteCarlo sampling of the trajectories with ends fixed in the initial and the target state, known as ‘Transition Path Sampling’ [3, 4, 5]. In practice, this means going from an ‘open-ended’ to a ‘two-ended’ procedure.

The purpose of this paper is to present a family of methods for the determination of reaction distributions and barriers. It is based on a dynamics that converges to barriers and reaction paths, much in the same way that diffusion in a potential converges to energy minima and metastable states. This allows us to construct ‘free energy barrier’ algorithms that can however be implemented in an open-ended manner.

The organization of this paper is as follows: in the first section we present the dynamics and we justify it in the second section.

DIFFUSION DYNAMICS AND PATH SAMPLING

Consider a Langevin process in an N -dimensional energy landscape $E(x_1, \dots, x_N)$:

$$\dot{x}_i = -E_i + \eta_i(t) \quad (1)$$

where $\eta(t)$ is a white noise of variance $2T$. Here and in what follows E_i and E_{ij} denote derivatives of E , $\partial_i \equiv \frac{\partial}{\partial x_i}$ and we adopt the summation convention. An equivalent way of stating (1) is to consider the probability distribution $P(x, t)$, evolving according to:

$$\frac{\partial P(x, t)}{\partial t} = -H_{FP} P(x, t) = -\partial_i J_i(x) \quad (2)$$

$$H_{FP} = -\partial_i (T \partial_i + E_i) \quad (3)$$

which defines the current $J_i(x, t) \equiv (T \partial_i + E_i) P(x, t)$.

The problem is how to modify (1) in order to devise a diffusive dynamics that targets saddle points and reaction paths. We shall show below that a set of N functions $R_i(\mathbf{x})$ evolving with

$$\frac{\partial R_i(x, t)}{\partial t} = -H_{FP} R_i(x, t) - E_{ij}(\mathbf{x}) R_j(x, t) \quad (4)$$

yields, at times $\tau_{fast} < t \ll \tau_{activ}$ a vector field $R_i(t) = J_i(\mathbf{x})$ describing reaction currents between metastable states — which one depends on the initial conditions. *In other words, (4) does for reaction paths what (2) does for states.*

Equation (4) is not immediately suitable for practical computations. Just as the natural way to simulate (2) is to use a diffusion dynamics (1), in order to have a practical approach we have to find the diffusion dynamics yielding (4).

Vector walkers. We consider a population of independent walkers $\mathbf{x}^a(t)$ carrying a vector internal degree of freedom $\mathbf{v}^a(t)$, an N -dimensional normalized vector. The dynamics consists of three types of transformations. Putting $A(\mathbf{x}^a) \equiv -v_i^a E_{ij} v_j^a$, they are :

- Ordinary diffusion of the positions $\mathbf{x}^a(t)$ as in (1);
- Length preserving rotation of the vector with a position-dependent rate: $\frac{dv_i^a}{dt} = -E_{ij} v_j^a(t) - A(\mathbf{x}^a) v_i^a$;

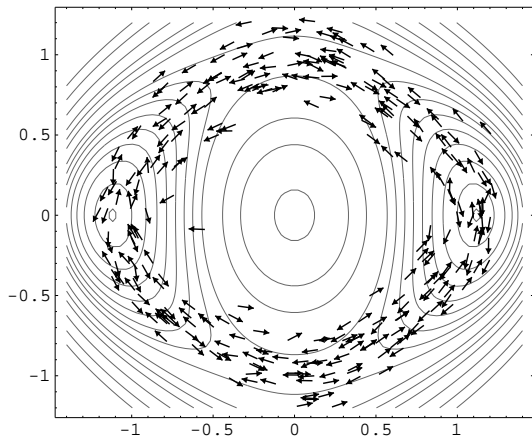


FIG. 1: Vector walkers describing a reaction path. The potential and the temperature are the ones of Ref. [3]. There are two minima at $(\pm\sqrt{5/4}, 0)$, two saddles at $(0, \pm 1)$ and a maximum at $(0, 0)$.

- Cloning with rate $A(\mathbf{x}^a)$ (if $A(\mathbf{x}^a) > 0$), or death with rate $-A(\mathbf{x}^a)$ (if $A(\mathbf{x}^a) < 0$). Clones are born in the same place with the same vector [11].

The rotation-cloning steps play the role of singling out the least stable direction, somewhat like in eigenvector-following and related methods [1, 2]. After a transient $\tau_{fast} < t \ll \tau_{activ}$, the system tends to a regime in which particles organize along trails: the reaction paths (Fig. 1). The distribution is almost stationary, there are regions of birth and emigration (near saddles) and regions of immigration and death (within the states). There is only a small global death rate of the order of the inverse reaction time along the specific path.

Denoting $F(\mathbf{x}, \mathbf{v}, t)$ the density of walkers, the current distribution is calculated from the average $R_i(\mathbf{x}, t) = \int d\mathbf{v} \mathbf{v} F(\mathbf{x}, \mathbf{v}, t)$. One can check that the R_i then satisfy (4), as desired. This algorithm can be seen as a Diffusion Monte Carlo as applied to (4) (see Refs. [6] and [7]).

Once an unnormalized transition current \mathbf{J} is known, the reaction time is obtained for example through:

$$\tau_{activ} = \frac{\int d\mathbf{x} e^{\beta E} |\mathbf{J}|^2}{\int d\mathbf{x} e^{\beta E} (\text{div} \mathbf{J})^2} \quad (5)$$

where $\beta = \frac{1}{T}$. The *barrier resistance* $e^{\beta E} |\mathbf{J}|^2$ is large in (and serves to indicate) barriers, while $e^{\beta E} (\text{div} \mathbf{J})^2$ is concentrated and essentially constant within the states involved in the passage [9]. In Fig. 2 we show the barrier resistance, as obtained from the present algorithm, for a purely entropic barrier.

Let us conclude by mentioning that sign problems are not *a priori* excluded here. They consist in the appearance of neighboring walkers with opposite vectors. For very low temperatures, and in particular for the evaluation of saddle-points, one can show [8] that this poses

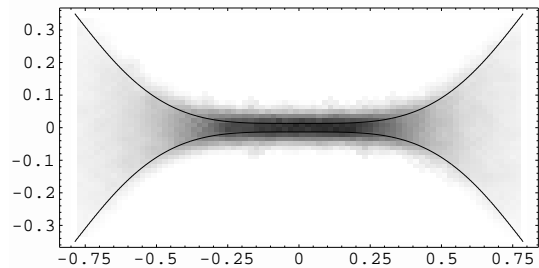


FIG. 2: Locating an entropic barrier with the vector walkers. The potential is flat between the two curves, and has steep harmonic walls. Darker regions correspond to larger values of the *barrier resistance* (see text).

no problem. Even at finite temperatures walker cancellations turn out not to be serious. However, one can always decimate the walkers, lumping them together according to the mean local orientation.

Transition path sampling with saddle-seeking paths. One can also use these ideas to improve transition path sampling [3, 4, 5]. This family of techniques involves sampling over trajectories, weighted with the appropriate action. In order to obtain information on reaction paths, it is necessary to force the ends of the trajectory to be at either side of a barrier — otherwise the trajectory collapses to a globular shape around one minimum.

If we wish the trajectory to seek for saddles, we need to add the effect of the second term on the rhs of (4). A simple calculation shows that this involves adding to the usual action a Lyapunov term equal to the logarithm of the largest eigenvalue of $U(t)$ defined from [12]:

$$\dot{U}_{ij} = -E_{ik} U_{kj} \quad (6)$$

(Adding in general the k -th eigenvalue makes the path seek the saddles with k unstable directions).

One can show that the path obtained with the Lyapunov term is concentrated with a density proportional to the barrier resistance $e^{\beta E} |\mathbf{J}|^2$ (cfr. Eq. (5)): thanks to this modification, if the trajectory is not constrained in any way, *it will spend its time near a barrier (even if entropic), and not in a state* (see Fig. 3), although the value of the action remains the same as for a pure Langevin weight. Thus the sampling can take better advantage of the regions that are difficult for the passage, also eliminating the problem of the large fluctuations associated with the jump time. If instead one end is tied to a minimum, the trajectory leaves the minimum and collapses to a globular shape around a nearby saddle (see Fig. 3): this can be used as a strategy to explore exit paths from a known configuration. The transition times in this setting can be calculated adapting the methods in [3].

THEORETICAL BACKGROUND

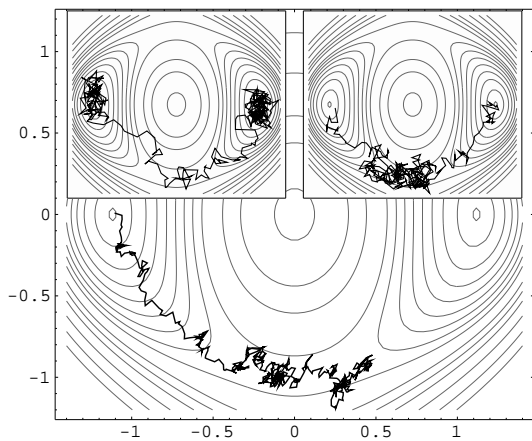


FIG. 3: Above: two-ended transition path sampling. Left: Langevin weight, right: Langevin + Lyapunov weight. Below: Langevin + Lyapunov action with only one end fixed while the other end is around a saddle. The potential is as in Fig. 1 [3].

To show these results, and to place them in a wider context, we introduce the supersymmetric formalism. Let us start by artificially ‘completing the square’ in (3) as follows: we introduce the N fermion creation and annihilation operators a_i and a_i^\dagger , with anticommutation relations $[a_i, a_j^\dagger]_+ = \delta_{ij}$, and define charges as:

$$\bar{Q} = -ia_i^\dagger(T\partial_i + E_i) \quad ; \quad Q = -iT a_i \partial_i \quad (7)$$

Both operators \bar{Q} and Q commute with H , are nilpotent $\bar{Q}^2 = Q^2 = 0$, and:

$$H = \frac{1}{T}(\bar{Q} + Q)^2 = H_{\text{FP}} + E_{ij} a_j^\dagger a_i \quad (8)$$

We consider a wave function $|\psi\rangle$ in the enlarged space and:

$$\frac{d|\psi\rangle}{dt} = -H|\psi\rangle \quad (9)$$

which yields a separate evolution for each fermion number subspace. The zero-fermion subspace is just the original space of probability distributions and (9) is the Fokker-Planck equation (3) for them. The one-fermion subspace is made of N -component functions $R_i(\mathbf{x})a_i^\dagger| \rangle$ ($| \rangle$ the fermion vacuum) and (9) reduces to (4) for them. More generally, the k -fermion subspace is spanned by $N!/k!(N-k)!$ functions.

As is well known, H_{FP} can be taken to a Hermitian form $H_{\text{FP}}^h = e^{\beta E/2} H_{\text{FP}} e^{-\beta E/2}$, and this is also true of H :

$$H_{\text{FP}}^h = \frac{1}{T} \sum_i \left[-T^2 \partial_i^2 + \frac{1}{4} E_i^2 - \frac{T}{2} E_{ii} \right] \quad (10)$$

$$H^h = e^{\beta E/2} H e^{-\beta E/2} = H_{\text{FP}}^h + E_{ij} a_j^\dagger a_i \quad (11)$$

The eigenvalue equations are:

$$H|\psi^{\mathbf{R}}\rangle = \lambda|\psi^{\mathbf{R}}\rangle \quad ; \quad H^h|\psi^{\mathbf{h}}\rangle = \lambda|\psi^{\mathbf{h}}\rangle$$

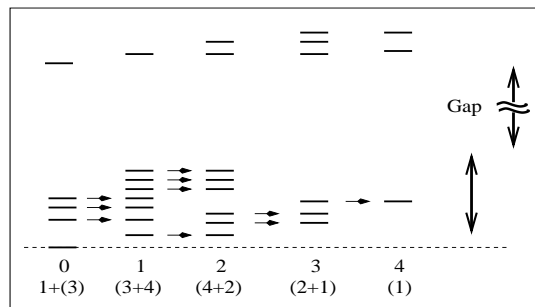


FIG. 4: Morse theory. The arrows indicate the action of \bar{Q} . The gap in the spectrum reflects timescale separation. The numbers between brackets indicate the number of states below the gap for each fermion number. The Morse inequalities can be read from the picture.

where

$$|\psi^{\mathbf{R}}\rangle = e^{-\beta E/2} |\psi^{\mathbf{h}}\rangle \quad (12)$$

Now, it is easy to see that applying Q to any eigenvector $|\psi^{\mathbf{R}}\rangle$ we get either a degenerate eigenvector with one less fermion, or zero. Similarly, applying \bar{Q} we get either a degenerate eigenvector with one more fermion or zero. Clearly, both Q and \bar{Q} annihilate the Gibbs measure. The spectrum is thus organized as in Fig 4.

The subspaces with non-zero fermion numbers are at this stage artificial. *The main result we need here is that small-eigenvalue (right) eigenvectors with one fermion encode the transition currents between states. On the other hand, small-eigenvalue k -fermion eigenvectors in the Hermitian base are peaked in all the saddle points with exactly k unstable directions.*

States. Before discussing transition distributions, we need to specify what we understand in general by ‘states’. In cases in which there is a timescale separation $\tau_{\text{fast}} \ll \tau_{\text{activ}}$, whatever its origin, the Fokker-Planck spectrum has a gap $\sim \tau_{\text{fast}}^{-1} - \tau_{\text{activ}}^{-1}$. Suppose there are K eigenvalues ‘below the gap’. An important and intuitive result due to Gaveau and Schulman [9] is that using linear combinations of them we can construct K distributions that are essentially Gibbsian in K disjoint regions, and elsewhere negligible. In other words, metastable states (up to a lifetime τ_{activ}) are linear combinations of states below the gap, and conversely. All these statements become sharper the larger the gap. The case of small temperatures is emblematic: the ‘states’ are simply narrow distributions (typically of width \sqrt{T}) peaked around local minima. This can be shown immediately from the low T expansion of (10).

Reaction Paths. Let us now sketch a proof of the fact that *one-fermion eigenvectors below the gap give the reaction-path distribution between states, and their times.* This means that Eq. (4) on times larger than τ_{fast} gives the reaction paths, and this in times much smaller than the passage-times τ_{activ} themselves.

Consider for simplicity the low-temperature situation, in which there are K minima separated by energy barriers, and a Langevin evolution starting from each minimum with a certain probability. If the time is of the order of the inverse of the largest passage time between any of the K states, there will be a current leaking through this saddle, and negligible flowing through all other paths (which take exponentially longer times). Next, consider times enough to allow the second fastest passage, there will be current flowing only through it: the faster reaction has already taken place (the states involved have mutually thermalized) and the slowest reactions-currents are exponentially smaller. If we continue this reasoning K times, each time allowing for a new activation, we obtain a sequence of K different linear combinations $\phi_K(\mathbf{x}), \dots, \phi_1(\mathbf{x})$ of the states below the gap, the last one $\phi_1(\mathbf{x})$ the Gibbs measure.

Consider next the $K - 1$ one-fermion right eigenvectors obtained acting with \bar{Q} on the $\phi_2(\mathbf{x}), \dots, \phi_K(\mathbf{x})$:

$$\bar{Q}\phi_a^L = (T\partial_i + E_i)a_i^\dagger\phi_a^L = J_i^a(x)a_i^\dagger| \rangle \quad (13)$$

From the preceding argument, they represent exactly $K - 1$ independent passage current distributions. Hence, in general each individual one-fermion eigenvector below the gap obtained as in (13) represents a passage current distribution with sources and sinks in the states (themselves defined as above). In the low temperature case, the distribution is non-negligible along a tube following ascending and descending gradient lines, passing through a barrier. The direction of $J_i^a(x)$ is parallel to the tube. The converse is also true: each passage between any two states is a linear superposition of these $K - 1$ currents.

In Fig. 4, we see that there are also one-fermion eigenvectors that are not the result of acting with \bar{Q} as in (13). They are characterized by being annihilated by Q , and this implies that they correspond to divergenceless current distributions. They are ‘tours’, for example an activated process leading from a minimum to itself through a saddle (think for example of a tilted Mexican hat). They are automatically distinguished in this formalism: for example (5) yields infinite timescales for them.

Hermitian base: saddles and Morse Theory.

One way to convince oneself that the formalism is a natural one is to see how it yields quite simply the topological relations between saddles (Morse theory). Let us review briefly the derivation in [10], specializing to the case of the topology of ordinary flat space and bounded systems. Consider the low temperature (harmonic) spectrum of (10): it is easy to show that k -fermion eigen-

vectors that have zero eigenvalue to leading order, are narrow Gaussians sitting on saddles with k unstable directions. This one-to-one relation between eigenfunctions ‘below the gap’ in the Hermitian base and saddles implies, as can be seen from Fig. 4 that there are relations between the numbers of saddles with successive numbers of unstable directions: $(1 + n_1), (n_1 + n_2), \dots, (n_{N-1} + n_N)$. The fact that $n_a > 0$ constitute the strong Morse inequalities for our case.

CONCLUSIONS

We described a family of methods to find transition paths and saddle points that, to the best of our knowledge, are quite different from the standards ones. The statement of the algorithms is simple, but the inspiration for them – and indeed the proof that they work – is based on the supersymmetric quantum mechanics construction, and its connection to Morse theory. Although we could not provide here many details of the derivations, and we have not yet performed tests in really hard cases, we hope we have argued convincingly that the tools are quite relevant for the problem [8].

Acknowledgments. We wish to thank N. Mousseau, W. Krauth, F. Schmüser and D. Wales for useful discussions.

-
- [1] D. J. Wales, *Energy Landscapes* (Cambridge University Press, 2003); D. J. Wales, A. M. Miller, and T. R. Walsh, *Nature* **394**, 758 (1998).
 - [2] N. Mousseau and G. T. Barkema, *Phys. Rev. E* **57**, 2419 (1998).
 - [3] C. Dellago, P. G. Bolhuis, F. S. Csajka, and D. Chandler, *J. Chem. Phys.* **108**, 1964 (1998).
 - [4] P. G. Bolhuis, D. Chandler, C. Dellago, and P. L. Geissler, *Annu. Rev. Phys. Chem.* **53**, 291 (2002).
 - [5] W. E, W. Ren, and E. Vanden-Eijnden, *Phys. Rev. B* **66**, 052301 (2002).
 - [6] S. Fahy and D. Hamann, *Phys. Rev. B* **43**, 765 (1991).
 - [7] S. Fantoni, A. Sarsa, and K. E. Schmidt, *Prog. Part. Nucl. Phys.* **44**, 63 (2000); K. E. Schmidt and S. Fantoni, *Phys. Lett. B* **446**, 99 (1999).
 - [8] S. Tănase-Nicola and J. Kurchan (unpublished).
 - [9] B. Gaveau and L. Schulman, *Jour. Math. Phys.* **39**, 1517 (1998).
 - [10] E. Witten, *J. Diff. Geom.* **17**, 661 (1982).
 - [11] Occasionally one must adjust the total number of walkers with a global death/birth rate.
 - [12] Note that this differs from the usual Lyapunov exponent that is defined considering $U^\dagger U$ — but one can that the eigenvalues of U are on average also positive.